

Coherent transport of single atoms in optical lattices

Wolfgang Merkel, Holger Mack, Matthias Freyberger, Victor V. Kozlov, and Wolfgang P. Schleich
Abteilung für Quantenphysik, Universität Ulm, Ulm, D-89069, Germany

Bruce W. Shore

618 Escondido Circle, Livermore, California 94550, USA

(Received 12 September 2005; published 28 March 2007)

We describe a technique for transferring a two-level atom between two adjacent potential wells of an optical lattice, using pairs of pump and Stokes pulses, each resonantly coupling the same pair of internal atomic states to form a Raman transition. Starting from a vibrational eigenstate of one well the atom slowly moves under the action of the pulse pair, to the vibrational eigenstate with the same quantum number in the neighboring well. The transfer takes place in two stages: A conventional stimulated Raman adiabatic passage (STIRAP) technique, in which Stokes precedes pump pulse, is followed by a pulse sequence where pump precedes Stokes and with an inverted sign of the Stokes envelope. In the first step the atom is accelerated toward the adjacent well and in the second step decelerated to the initial vibrational energy. The STIRAP technique avoids the introduction of stochastic motion caused by spontaneous emission from the excited internal atomic state.

DOI: [10.1103/PhysRevA.75.033420](https://doi.org/10.1103/PhysRevA.75.033420)

PACS number(s): 32.80.Lg, 32.80.Qk, 32.80.Pj

I. INTRODUCTION

Recent advances in cooling atoms have boosted technological developments in the creation and manipulation of optical lattices [1,2]. Nowadays, a wide variety of optical lattices have been realized by combining counterpropagating electric fields to form a standing light wave in one, two, or three dimensions [3]. The problem of coherent control of atomic motion comes now on the forefront. The transfer of a single atom through the optical lattice constitutes the main subject of this work.

The scattering force exerted on an atom by the electric field cools the motion of the atom and the dipole force keeps the atom trapped in optical lattices. The parameters of optical lattices can be controlled relatively easy. By varying frequency, phases and intensity of the electric fields and optionally applying auxiliary magnetic fields, one can manipulate the depth of the optical potential, its shape, and relative values of dipole and scattering forces. An atom can be cooled to the vibrational ground state [4] which is a convenient starting point for the preparation of a Fock state with a higher quantum number in optical lattices [5] or the generation of a wave packet [6].

Atoms in an optical lattice bear a close analogy to electrons in a crystal. As a favorable feature, the interatomic spacing in an optical lattice is of the order of micrometers as compared to the nanometer scale characteristic for solids. The large atom separation allows one to study the dynamics of particles in periodic structures in the regime of weak interactions, which is hard to achieve in solid matter. Optical lattices and the associated field of atomic physics have already demonstrated the potential to serve as ideal testing ground for studying phenomena that are traditionally attributed to solid state physics. Thus, effects like Bloch oscillations and quantum transport usually spoiled by impurities and defects present in solids, were opened for a clear observation by use of atoms trapped in an optical lattice [7,8]. The generation of nanoscale structures in atom lithography [9], implementation of scalable quantum logic [10,11], controllable playground for the observation of Lévy flights [12,13] are yet other applications of optical lattices.

Further developments in optical lattice technology depend on the ability to vary the local density of the atoms, and ideally control the position of single atoms. Atoms can be transported through the lattice in a number of ways: by tunneling [14], by directed diffusive transport in asymmetric [15] and symmetric [16] optical lattices, as recently demonstrated by coherent spin-dependent transfer [17], and by the optical conveyor belt technique [18]. However, these approaches to quantum transport are either of statistical nature, without precise control over the atomic motion, or collective in nature, in the sense that many atoms throughout the optical lattice are affected simultaneously, all together. We propose here a method which allows to address an *individual* atom and *deterministically* move it through the lattice.

Our paper is organized as follows: In Sec. II we overview the quantization of the atomic center-of-mass motion in the optical lattice and, assuming a deep optical potential, describe the confined atomic motion inside each potential by a set of Wannier states. In Sec. III we treat the atom as a two-level system and consider its resonant interaction with Stokes and pump light fields; then we further restrict our attention to one period of the optical lattice and derive a three-well model describing the motion of the two-level atom under the action of the two pulses in a Raman configuration. In Sec. IV we sketch the basics of a three-state Λ model driven by the Raman pair and concentrate on the STIRAP technique as an attractive method for complete population transfer which is not accompanied by a spontaneous decay from the upper state. In Sec. V we reduce the three-well model to an effective five-state scheme and modify the conventional three-state STIRAP technique to achieve a desirable population dynamics that is equivalent to the transfer of the atom to an adjacent potential well. In Sec. VI we conclude with a discussion of the atomic motion under the action of resonant Raman pulses and speculate on possible generalizations of the proposed method for the atom transport.

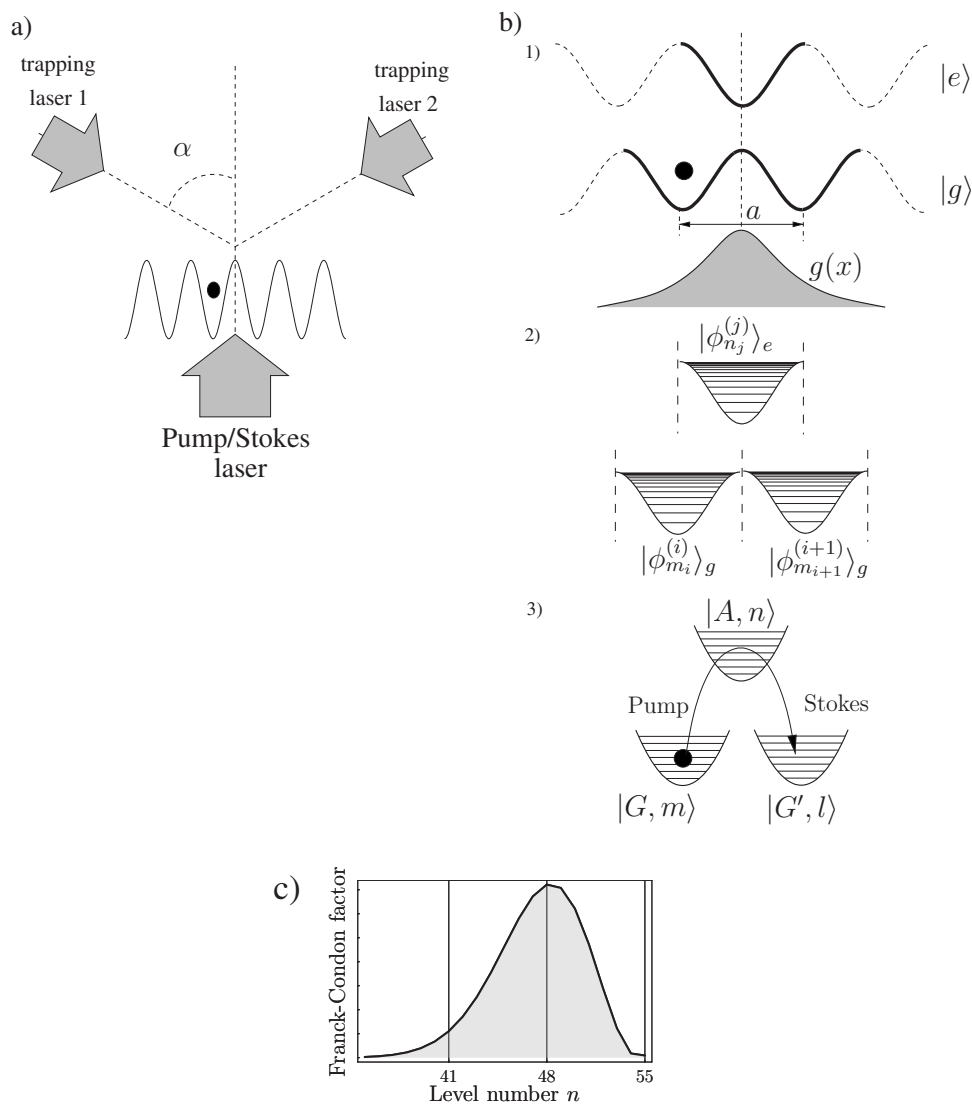


FIG. 1. Coherent transport of an atom in an optical lattice due to a Raman pulse. (a) Sketch of the generic setup. The optical lattice of period a , Eq. (1), is created by two laser beams 1 and 2 propagating and crossing at angle 2α . Application of the pump and Stokes pulses produces a force which moves the atom from the left lattice site to the right one. (b) Quantization of the atomic motion in the optical lattice. (1) The state selective optical potential, Eq. (2). The potential for the atom in the excited state is shifted by $a/2$ with respect to the potential for the atom in the ground state. The driving lasers with transverse profile $g(x)$ illuminate predominantly one period (a) of the optical lattice. In bold are shown three potential wells involved in the transfer, two in the atomic ground state $|g\rangle$ and one in the excited state $|e\rangle$. For better selectivity the transverse beam shape $g(x)$ should be chosen with flat top and steep wings like a super-Gaussian shape. (2) Quantization of the atomic center of mass motion within each lattice site. Dashed vertical lines indicate that each well is treated separately. (3) Approximation of each \sin^2 -shape well by a truncated parabola. Corresponding harmonic oscillator energy levels are shown by horizontal equidistant lines. The Raman pump-Stokes pair of pulses realizes the transfer. (c) The Franck-Condon factors $d_{\bar{m}n}^2 = \langle G, \bar{m} | A, n \rangle^2$ calculated as the transition matrix elements from the chosen vibrational state $\bar{m}=43$ in the left manifold to a number of vibrational states in the excited manifold; see Eq. (38). The factors are evaluated in the harmonic approximation where the harmonic potential matches the \sin^2 potential in the vicinity of the central eigenstate $|G, \bar{m}\rangle$.

II. QUANTIZATION OF THE CENTER-OF-MASS MOTION OF A TWO-LEVEL ATOM

We consider a two-level atom of mass M_0 with ground state $|g\rangle$ and excited state $|e\rangle$ interacting with the off-resonant standing wave generated by the two trapping laser beams 1 and 2, both of wavelength λ and Rabi frequency Ω_{OL} detuned from the atomic transition by Δ_{OL} ; see Fig. 1(a). The two beams propagate at angle 2α with respect to each other and form a standing wave in the horizontal direction, the

configuration used for example in Ref. [5] to prepare Fock states of neutral atoms. The spatial period of the standing wave is

$$a = \frac{\lambda}{2 \sin \alpha}. \quad (1)$$

For the case of most common configuration, i.e., $\alpha = \pi/2$, the counterpropagating beams form the one-dimensional stand-

ing wave with the period of $\lambda/2$. The atom experiences the optical lattice as an effective potential

$$U(x) = U_0 \sin^2\left(\frac{\pi x}{a}\right) (|g\rangle\langle g| - |e\rangle\langle e|), \quad (2)$$

where $U_0 = \hbar\Omega_{\text{OL}}^2/\Delta_{\text{OL}}$ is the depth of the optical potential. The potential

$$U(x+a) = U(x) \quad (3)$$

is a periodic function with period a .

The potential is state-selective as it depends on the electronic state of the atom: The potential for the atom in the excited state is shifted by $a/2$ with respect to the potential for the atom in the ground state. The (trapping) Hamiltonian for the atomic center-of-mass motion in an optical lattice is given by

$$H_0 = \frac{p^2}{2M_0} + U(x). \quad (4)$$

With this Hamiltonian, Eq. (4), in the Schrödinger equation we approach the quantization of the atomic center-of-mass motion. The problem is solved when the eigenvalues and corresponding eigenfunctions of operator H_0 are found. For an arbitrary potential, the energy eigenvalues can be classified in two groups: The continuous and the discrete spectrum. Since the operator is Hermitian, eigenfunctions of H_0 form a complete set. Therefore, the evolution of a given initial wave function can be described in terms of an expansion in the basis of energy eigenfunctions with time dependent probability amplitudes.

We consider an optical lattice with deep modulation U_0 . For such a potential the energy spectrum consists of energy bands of allowed energies which are separated by gaps of forbidden energies. The width of these energy bands is closely related to the tunneling rate between neighboring potential wells: The larger the tunneling rate the broader the width of the bands. For small energies the potential barrier is relatively thick so that the tunneling is vanishingly weak. Therefore the width of such bands vanishes and thus resembles the discrete spectrum of an atom in a single potential well. For the problem of atom transport we use energy bands at the level of $U_0/2$. For the deep potential they are quite narrow and will be treated as discrete states in the following. Physically this approximation means that the characteristic evolution time of the atom is much faster than the inverse bandwidth of each involved band. In other words, we observe the evolution of the atom on a time scale shorter than compared to the tunneling time. For higher energies (approaching U_0 and above) the tunneling rate is larger and the associated bands are broader.

An atom trapped in an optical lattice bears close analogy to the motion of an electron in a periodic potential of a solid state crystal. Two alternative approaches are used to describe the electronic motion. For electrons characterized by relatively high energies the wave function is conveniently described as a superposition of Bloch waves. Bloch waves are extended over the whole crystal and periodically modulated with the period of the crystal. Alternatively, for lower ener-

gies when the electronic wave function is confined to a single lattice site, a description in terms of Wannier states becomes favorable. Wannier states are energy eigenstates of the potential of a single lattice site. Since the spatial width of the Wannier states does not exceed the width of the lattice site, Wannier states belonging to different sites are orthogonal. The Wannier approach is clearly correlated with the no-tunneling approximation for low-lying states, discussed in the previous paragraph. Since the vibrational states of interest have energies in the vicinity of $U_0/2$ we will follow the Wannier approach throughout the paper.

With the no-tunneling approximation we reduce the periodic potential to a sequence of independent wells according to

$$U(x) = \sum_i V_g^{(i)}(x) |g\rangle\langle g| + \sum_j V_g^{(j)}(x) |e\rangle\langle e|, \quad (5)$$

where $V_g^{(i)}(x)$ [$V_e^{(j)}(x)$] is the potential restricted to a single lattice site i (j) in the ground (excited) state. Here x runs from $-a/2$ to $a/2$. The translational invariance of the optical potential allows us to trace each single-well potential

$$V_g^{(i)}(x) = V_g^{(0)}(x - ia), \quad (6)$$

$$V_e^{(j)}(x) = V_g^{(0)}\left(x - (2j+1)\frac{a}{2}\right) \quad (7)$$

back to the single potential well $V_g^{(0)}(x) \equiv V(x)$ centered in the origin. The atomic motion in the central lattice site [and according to Eqs. (6) and (7) in all other sites] is governed by the single-well Hamiltonian

$$H_{00} \equiv \frac{p^2}{2M_0} + V(x). \quad (8)$$

The quantization of the center-of-mass motion in the central lattice site corresponds to the eigenstate problem

$$H_{00}|\phi_k\rangle = \hbar\omega_k|\phi_k\rangle. \quad (9)$$

Thus we get a manifold of energy eigenstates $|\phi_k\rangle$ each characterized by energy $\hbar\omega_k$. Note that our interest is only in eigenstates with energies below U_0 , since only they possess the characteristic property of Wannier states.

In order to characterize atomic states for the entire lattice we introduce the following notations. For the atom in the ground internal state and n_i th Wannier state belonging to i th lattice site we use notation $|\phi_{n_i}^{(i)}\rangle_g$. Analogously, we denote by $|\phi_{m_j}^{(j)}\rangle_e$ the atom in the excited internal state characterized by m_j th vibrational eigenstate located in the j th lattice site. The associated energy eigenvalues are $\hbar\omega_{g,i,n_i}$ and $\hbar\omega_{e,j,m_j}$, respectively.

Wannier states belonging to same internal state $l=g, e$ are orthogonal

$$\langle\phi_{n_i}^{(i)}|\phi_{n_k}^{(k)}\rangle_l = \delta_{ik}\delta_{n_i n_k}. \quad (10)$$

We use Wannier states of all lattice sites to form a complete set

$$1 = \sum_i \sum_{n_i=0}^M |\phi_{n_i}^{(i)}\rangle_g \langle \phi_{n_i}^{(i)}| + \sum_j \sum_{m_j=0}^M |\phi_{m_j}^{(j)}\rangle_e \langle \phi_{m_j}^{(j)}|. \quad (11)$$

Here indices i and j span over all lattice sites. Quantum numbers n_i and m_j have upper bound M , where M is the number of Wannier states which are localized within one lattice site.

Formally, the completeness relation implies that at all times (in all wells) the atomic wave function can be described as superposition

$$|\Psi(t)\rangle = \sum_i \sum_{n_i=0}^M \alpha_{g,n_i}^{(i)} |\phi_{n_i}^{(i)}\rangle_g + \sum_j \sum_{m_j=0}^M \beta_{e,m_j}^{(j)} |\phi_{m_j}^{(j)}\rangle_e, \quad (12)$$

where $\alpha_{g,n_i}^{(i)}(t)$ and $\beta_{e,m_j}^{(j)}(t)$ are the time-dependent probability amplitudes for finding the atom in the Wannier states $|\phi_{n_i}^{(i)}\rangle_g$ and $|\phi_{m_j}^{(j)}\rangle_e$, respectively.

At this stage there is no need to specify energy eigenfunctions of a single well of \sin^2 -shape potential. The explicit form of Wannier states becomes important when we arrive at the explicit calculation of the coupling matrix elements (Franck-Condon factors). There we find it useful to apply a harmonic approximation.

III. ATOM TRANSPORT: DERIVATION OF THE MODEL

A. Interaction of the trapped atom with optical fields

The trapped atom is now illuminated by a pair of resonant fields with the aim to drive the atom from one to the adjacent potential well. The total Hamiltonian of the system is the sum $H \equiv H_0 + W$ of the Hamiltonian of the trapped atom Eq. (4) and the interaction term $W \equiv -d\mathcal{E}(t)$ describing the dipole interaction of the atom with the resonant field $\mathcal{E}(t)$. The Hamiltonian H_0 is decomposed in terms of Wannier states

$$H_0 = \hbar \sum_i \sum_{n_i=0}^M \omega_{g,i,n_i} |\phi_{n_i}^{(i)}\rangle_g \langle \phi_{n_i}^{(i)}| + \hbar \sum_j \sum_{m_j=0}^M \omega_{e,j,m_j} |\phi_{m_j}^{(j)}\rangle_e \langle \phi_{m_j}^{(j)}|, \quad (13)$$

using the completeness relation Eq. (11). The interaction term is expanded as

$$W = - \sum_{i,j} \sum_{n_i,m_j=0}^M (\varphi_{n_i,m_j}^{(i,j)} |\phi_{n_i}^{(i)}\rangle_g \langle \phi_{m_j}^{(j)}| + \varphi_{m_j,n_i}^{(j,i)} |\phi_{m_j}^{(j)}\rangle_e \langle \phi_{n_i}^{(i)}|) \mathcal{E}(t), \quad (14)$$

with coupling matrix elements

$$\varphi_{n_i,m_j}^{(i,j)} = \mathcal{D}_{ge} \langle \phi_{n_i}^{(i)} | \phi_{m_j}^{(j)} \rangle_e = (\varphi_{m_j,n_i}^{(j,i)})^*. \quad (15)$$

Here we used the fact that the dipole operator acts only on the internal degrees of freedom and introduce the dipole matrix element $\mathcal{D}_{ge} = \langle g | d | e \rangle$. In Eq. (15) we introduced the Franck-Condon factor as the overlap of the two Wannier states. Note that the separation of the atomic dynamics in the motion of the center-of-mass and the electronic degrees of

freedom becomes possible due to the distinct time scales of the two processes (Franck-Condon principle).

The electric field

$$\mathcal{E}(t) = \sum_{k=P,S} [E_k(t) e^{-i\omega_k t} + \text{c.c.}] \quad (16)$$

is the combination of two narrowband optical fields, Stokes and pump, centered at carrier frequencies ω_S and ω_P .

In the interaction picture, the evolution of the wave function is described by the Schrödinger equation

$$i\hbar \frac{\partial}{\partial t} |\Psi(t)\rangle = \mathcal{W} |\Psi(t)\rangle \quad (17)$$

with the interaction Hamiltonian transformed to the interaction picture according to $\mathcal{W} = \exp[(i/\hbar)H_0 t] W \exp[-(i/\hbar)H_0 t]$. Substituting the wave function in the form of the decomposition Eq. (12) into the Schrödinger equation Eq. (17), performing projections with the help of the orthogonality relation Eq. (10), and applying the rotating wave approximation we get equations of motion for the probability amplitudes:

$$i\hbar \frac{d}{dt} \alpha_{g,n_i}^{(i)} = \sum_{k=P,S} E_k \sum_j \sum_{m_j=0}^M \varphi_{n_i,m_j}^{(i,j)} e^{-i(\omega_{e,j,m_j} - \omega_{g,i,n_i} - \omega_k)t} \beta_{e,m_j}^{(j)}, \quad (18)$$

$$i\hbar \frac{d}{dt} \beta_{e,m_j}^{(j)} = \sum_{k=P,S} E_k^* \sum_i \sum_{n_i=0}^M (\varphi_{n_i,m_j}^{(i,j)})^* e^{+i(\omega_{e,j,m_j} - \omega_{g,i,n_i} - \omega_k)t} \alpha_{g,n_i}^{(i)}. \quad (19)$$

Recall that indices i and j label the site of the optical lattice, whereas the n_i and m_j denote the quantum number of the corresponding Wannier state.

This system of coupled equations allows us to follow the evolution of the atomic function under the action of the Stokes and the pump field. In particular, it is possible to drive the atom through the optical lattice. In the next sections we suggest a sequence of pulses which performs such a transfer. Before doing this we reduce the general set of equations (18) and (19) to a three-well model.

B. Three-well model

The transfer is accomplished by applying the pump and Stokes pulses in a Raman configuration with intermediate resonant coupling to the excited state. Only one period of the optical lattice is illuminated by the spatially confined laser pulses of transverse profile $g(x)$, as depicted in Fig. 1(b). Due to the finite spatial profile strong coupling is established between wells belonging to the illuminated double well structure. In contrast, adjacent lattice sites interact with the tails of the pulses where the electric field vanishes and therefore they appear to be only weakly exposed to the transport laser pulses. In the following we neglect these weak couplings [19]. In order to illuminate only one lattice period in the counterpropagating configuration ($\alpha = \pi/2$) one needs to focus the trapping beams to a spot of the size close to the

diffraction limit. In order to ease this tight focusing requirement the spot can be made twice bigger for $\alpha = \pi/6$.

Only atoms located in the two selected sites are thus addressed by the pulses. For definiteness, let us assume that we have only one atom which is located in the left well. Then, the geometry imposes the direction of the transfer process: From the left to right well in our case. Only two wells ($i = 0, 1$) in the ground state and one well ($j = 0$) in the excited state are involved in the dynamics. The corresponding probability amplitudes are denoted according to the following scheme

$$\text{left well: } \alpha_{n_0}^{(0)} \rightarrow G_n, \quad (20)$$

$$\text{right well: } \alpha_{n_1}^{(1)} \rightarrow G'_l, \quad (21)$$

$$\text{upper well: } \beta_{m_0}^{(0)} \rightarrow A_m, \quad (22)$$

whereas the associated Wannier states are relabeled according to

$$|\phi_{n_0}^{(0)}\rangle_g \rightarrow |G, n\rangle, \quad (23)$$

$$|\phi_{n_1}^{(1)}\rangle_g \rightarrow |G', l\rangle, \quad (24)$$

$$|\phi_{m_0}^{(0)}\rangle_e \rightarrow |A, m\rangle. \quad (25)$$

The energy eigenvalues are replaced according to

$$\hbar\omega_{g,0,n_0} \rightarrow \hbar\omega_{G,n}, \quad (26)$$

$$\hbar\omega_{g,1,n_1} \rightarrow \hbar\omega_{G',l}, \quad (27)$$

$$\hbar\omega_{e,0,m_0} \rightarrow \hbar\omega_{A,m}. \quad (28)$$

Within the three-well model the equations of motion Eq. (18) and Eq. (19) reduce to

$$i\hbar\dot{G}_n = \sum_{k=P,S} E_k \sum_{m=0}^M d_{nm} e^{-i\Delta_{mn}^{(k)} t} A_m, \quad (29)$$

$$i\hbar\dot{A}_m = \sum_{k=P,S} E_k \left(\sum_{n=0}^M d_{nm}^* e^{i\Delta_{mn}^{(k)} t} G_n + \sum_{l=0}^M \bar{d}_{lm} e^{i\Delta_{ml}^{(k)} t} G'_l \right), \quad (30)$$

$$i\hbar\dot{G}'_l = \sum_{k=P,S} E_k \sum_{m=0}^M \bar{d}_{lm} e^{-i\Delta_{ml}^{(k)} t} A_m, \quad (31)$$

with detunings $\Delta_{nm}^{(k)} = \omega_{A,m} - \omega_{G,n} - \omega_k$ and $\Delta_{ml}^{(k)} = \omega_{A,m} - \omega_{G',l} - \omega_k$, and dipole moments $d_{nm} = \varphi_{n,m}^{(0,0)}$ and $\bar{d}_{lm} = \varphi_{l,m}^{(1,0)}$.

The set of equations (29)–(31) takes into account all possible transitions between vibrational states belonging to all three potential wells of interest. These transitions are of two types. The first type describes the desirable interwell transfer of the atom. The second (undesirable) type of transition connects vibrational states of the same well and thereby de-

scribes Raman-induced heating processes. Later we find that for our choice of Stokes and the pump pulses such heating processes are negligible.

Starting with the atom in the well $|G\rangle$ our goal is to transfer it to the adjacent well $|G'\rangle$, as illustrated in Fig. 1(b). The atom is initially prepared in the motional state $|G, \bar{n}\rangle$ with probability equal to unity. Two fields E_P and E_S are applied to shift the atom to the right well. We consider the transfer to be successful if the probability of the atom to appear in the right well is close to unity. The most desirable arrangement of the fields is such that the atom is transferred to a single vibrational eigenstate, say $|G', \bar{l}\rangle$. Then, taking this state as a new initial condition the transfer scheme can be repeated again along similar lines.

The efficiency of couplings between the vibrational states of the lower and the excited manifold is evaluated as overlap integrals of the corresponding Wannier function $\langle x|G, n\rangle$ ($\langle x|G', l\rangle$) of the n th (l th) vibrational state in the left (right) potential well and $(a/2)$ -shifted Wannier function $\langle x|A, m\rangle$ of the m th vibrational state in the upper manifold. Thus, for a transition from a given state $|G, n\rangle$ in the left manifold to a state $|A, m\rangle$ in the upper manifold the dipole moment d_{nm} defined by Eq. (15) is proportional to the Franck-Condon factor

$$\langle G, n|A, m\rangle = \int_{-\infty}^{+\infty} dx \langle x|G, n\rangle^* \langle x|A, m\rangle. \quad (32)$$

C. Evaluation of Franck-Condon factors

So far, we did not need an explicit form of the Wannier functions. Now, for the evaluation of the Franck-Condon factors we simplify the model of each well. We approximate each of the three wells of the \sin^2 potential by a harmonic oscillator potential $\frac{1}{2}M_0\nu^2$ and use only eigenfunctions with energies below U_0 , as illustrated in Fig. 1(b). Initially the atom has well-defined energy at approximately half U_0 . Therefore it is more reasonable to make the parabolic fit of the \sin^2 potential at energies corresponding to $U_0/2$ rather than in the minimum. The fitting parameters are the zero-energy shift $\Delta U = (U_0/2)(1 - \pi/4)$ and the trap frequency

$$\nu = \frac{2}{a} \sqrt{\frac{\pi U_0}{M_0}}, \quad (33)$$

which determines the energy separation $\hbar\nu$ of eigenstates of the harmonic oscillator. Energy eigenvalues $\hbar\omega_{G,n}$ in the left well are replaced by $\hbar\nu(n + \frac{1}{2})$. Analogously in the other two wells, we replace $\hbar\omega_{G',l}$ and $\hbar\omega_{A,m}$ by correspondingly $\hbar\nu(l + \frac{1}{2})$ and $\hbar\nu(m + \frac{1}{2})$. For all three potential wells we find the real-valued eigenfunctions

$$u_k(x) = \left(\frac{\kappa^2}{\pi}\right)^{1/4} \frac{e^{-(\kappa x)^2/2}}{\sqrt{2^k k!}} H_k(\kappa x), \quad (34)$$

of the harmonic oscillator with characteristic length scale $\kappa^{-1} \equiv \sqrt{\hbar/M_0\nu}$, where the quantum number k has to be replaced by n, l , or m depending on the particular potential well under consideration.

Note that only harmonic oscillator eigenfunctions $u_k(x)$ with energies less than U_0 are localized within a primitive cell of the optical lattice. Assuming that the eigenfunction $u_{\bar{M}}(x)$ with quantum number \bar{M} reaches the spatial size of a single lattice site we truncate here the set of harmonic oscillator eigenfunctions. Thus $u_k(x)$ with k running from 0 to \bar{M} form a suitable set of Wannier functions for each potential well under consideration. The truncated sets for all lattice sites spatially cover the entire lattice and therefore all together represent the basis.

Then, in position representation, the Wannier functions become

$$\langle x|G, n\rangle = u_n(x), \quad (35)$$

$$\langle x|A, m\rangle = u_m\left(x - \frac{a}{2}\right), \quad (36)$$

$$\langle x|G', l\rangle = u_l(x - a), \quad (37)$$

where indices n , m , and l run from 0 to \bar{M} . The dipole moments for the excitation step become then

$$d_{nm} = \mathcal{D}_{ge}\langle G, n|A, m\rangle = \mathcal{D}_{ge} \int_{-\infty}^{+\infty} dx u_n(x)u_m(x - a/2), \quad (38)$$

whereas for the deexcitation step we get

$$\bar{d}_{ml} = \mathcal{D}_{ge}\langle A, m|G', l\rangle = \mathcal{D}_{ge} \int_{-\infty}^{+\infty} dx u_m(x - a/2)u_l(x - a). \quad (39)$$

The parity of the harmonic oscillator eigenfunctions in Eq. (34) is a function of the quantum number k . If the vibrational eigenstates with quantum number n of the two lower wells have the same parity as an eigenstate with quantum number m in the upper well, then the dipole moments for excitation and deexcitation step are equal: $d_{nm} = \bar{d}_{nm}$. Otherwise, we find $d_{nm} = -\bar{d}_{nm}$. These two equalities are summarized by

$$d_{nm} = (-1)^{n+m} \bar{d}_{nm}. \quad (40)$$

Figure 1(c) shows the Franck-Condon factors evaluated in the harmonic approximation. Here values of $d_{\bar{n}m}^2$ are depicted characterizing the strength of the transition from the initial state $|G, \bar{n}\rangle$ with energy $U_0/2$ to a number of states $|A, m\rangle$ in the upper well.

D. Atom transport

In order to improve the coupling efficiency the overlap integral in Eq. (38) has to be maximized. According to the Franck-Condon principle, the integral reaches the greatest value for transitions between the states whose classical turning points can be connected by a vertical line. This guiding rule helps us to draw an important conclusion. Since the

lower and excited manifolds are shifted with respect to each other, the atom, when excited from the ground state, can end up very close to the continuum of states. Here the atom appears to be trapped rather weakly and acquires some undesirable probability to escape the coherent control. In order to preserve the deterministic character of the transfer process the atom is prepared in a single vibrational state with the energy corresponding to half the potential depth and with quantum number \bar{m} . Franck-Condon factors for transitions from the state $|G, \bar{m}\rangle$ to a number of states in the excited manifold are presented in Fig. 1(c). Note that the transfer schemes presented below are not sensitive to the particular choice of the initial state. Other eigenstates (apart from those characterized by very low and very high quantum numbers) are equally well suited as initial conditions.

Two factors determine the number of states participating in the dynamics. First is the value of the Franck-Condon factors and thereby the strength of applied fields. The second factor is the degree of monochromaticity of the pump and the Stokes fields. It is determined by the relation of the pulses' bandwidth $\Delta\omega$ and the characteristic frequency difference between two adjacent vibrational states ν . Thus, we can account for the bandwidth dependence by introducing the parameter

$$R = \frac{\Delta\omega}{\nu}. \quad (41)$$

The smaller the R parameter the better the degree of monochromaticity of the fields. In order to preserve the eigenstate character of the final state we shall keep R small.

It is not simple to determine the number of states coupled by two fields E_P and E_S . The structure of equations of motion Eqs. (29)–(31) implies that the pump and the Stokes fields couple both right and left manifolds to the manifold of excited states. Therefore, the situation is more complicated than the usual Raman configuration shown in Fig. 1(c). The picture becomes realistic when supplemented with the Stokes field coupling the left and the upper manifold and correspondingly with the pump field coupling the right and the upper manifold. Moreover, for sufficiently deep potential wells, vibrational states are equidistant to a good approximation and therefore the resonant coupling takes place between a vast number of vibrational states from both, right and left, manifolds to corresponding states in the upper manifold.

We shall see that this complicated ladder of cross-couplings can be reduced to a tractable scheme by a judicious choice of frequencies of applied fields based on the nonuniformity of the distribution of Franck-Condon factors; see Fig. 1(c). Note that the equations of motion, Eqs. (29)–(31), put on equal footing the control of atomic center-of-mass motion and the nonlinear-optical problem of the dynamics of an electron bound to an atom and driven by external fields. For the latter, methods are known on how to transfer the electron to a given quantum state. We start with overviewing existing concepts and use them as the basis for our scheme.

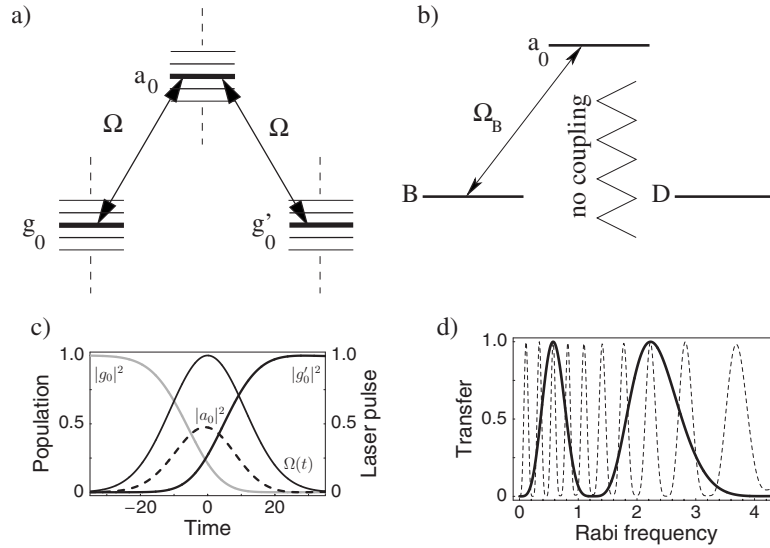


FIG. 2. Atom transport as viewed in the language of a degenerate Λ system. (a) Level structure of Fig. 1(b) showing a few relevant neighboring states around central states $|G, \bar{m}\rangle$, $|A, \bar{n}\rangle$, and $|G', \bar{m}\rangle$ denoted by the corresponding probability amplitudes g_0 , a_0 , and g'_0 . (b) Dressed state picture of the Λ system composed of central states g_0 , a_0 , and g'_0 . In bare state basis fields Ω_P and Ω_S have the same frequency and are therefore indistinguishable. In the dressed state picture the indistinguishability appears as the single bright field Ω_B coupling a_0 and B , while the dark state D stays fully decoupled. (c) Evolution of populations $|g_0|^2$, $|a_0|^2$, and $|g'_0|^2$ of the three central states under the action of a Gaussian pulse $\Omega(t) = \Omega_0 \exp[-t^2/2\Delta t^2]$ using the relation $\Delta t = (R\nu)^{-1}$ between the temporal width Δt and the nonmonochromaticity parameter R . Parameters are nonmonochromaticity parameter $R=0.1$ and peak Rabi frequency $\Omega_0=0.28$. From here on time and Rabi frequency are given in units of the vibrational period $T \equiv 2\pi/\nu$ and $1/T$, respectively. Note that the complete population transfer to the target state g'_0 is accompanied by a substantial transit of population through the excited state a_0 . (d) Final (after the passage of the Raman pulse) population $|g'_0|^2$ of the target state as a function of peak Rabi frequency for two values of R . Well pronounced Rabi oscillations are obtained for $R=0.02$ (dashed line) over a wide range of Rabi frequencies, whereas for larger pulse bandwidth ($R=0.1$, solid line) the oscillations degrade fast.

IV. Λ PHYSICS

The structure of equations of motion Eqs. (29)–(31) implies that at least three states, one per each well, are coupled by the pump and the Stokes fields. Therefore, we take the three-level Λ configuration as starting point of our analysis. A necessary (but not sufficient) condition for the three-level approximation is that the fields are applied in the form of long pulses such that the R parameter is sufficiently small. We postpone to a later section the question of when and in what sense a three-level model can provide a realistic description of the transfer. In this section we introduce two types of Λ systems distinguished by the carrier frequency of the fields in the Raman pair. If they are equal, then the fields are indistinguishable and form the scheme called degenerate Λ system. Otherwise, the case is classified as the nondegenerate Λ system.

The three states participating in the transfer are denoted by $|G, \bar{m}\rangle$, $|A, \bar{n}\rangle$, and $|G', \bar{l}\rangle$. They are chosen without particular reference to the transfer scheme. However, for definiteness, in the following numerical examples we shall specify the involved quantum numbers explicitly. Two other relevant quantities are Rabi frequencies of the pump and Stokes fields. They are introduced as $\Omega_P = d_{\bar{m}\bar{n}} E_P / \hbar$ and $\Omega_S = d_{\bar{l}\bar{n}} E_S / \hbar$, correspondingly.

A. Degenerate Λ scheme

We identify two possible types of the Λ configuration. First, and most simple, is the degenerate case when the two

chosen states in the left and right manifold are characterized by equal quantum numbers $\bar{m} = \bar{l}$. Then, resonant transitions are characterized by equal frequencies and thus the pump and Stokes fields become indistinguishable. They can be replaced by a single field with Rabi frequency $\Omega = \Omega_P = \Omega_S$. The equations of motion for this configuration are deduced from the main set of equations, Eqs. (29)–(31), by keeping only one term in each sum. In new notations we get

$$i \frac{d}{dt} \begin{pmatrix} g_0 \\ a_0 \\ g'_0 \end{pmatrix} = \frac{1}{2} \begin{pmatrix} 0 & \Omega & 0 \\ \Omega & 0 & \Omega \\ 0 & \Omega & 0 \end{pmatrix} \begin{pmatrix} g_0 \\ a_0 \\ g'_0 \end{pmatrix}, \quad (42)$$

where g_0 , a_0 , and g'_0 are probability amplitudes belonging to the three states $|G, \bar{m}\rangle$, $|A, \bar{n}\rangle$, and $|G', \bar{m}\rangle$; correspondingly, see Fig. 2(a). Although we take $\bar{m} = \bar{l}$, the methods presented below are not sensitive to a particular choice of the set of three levels as long as transitions are not forbidden or heavily suppressed by the structure of the Franck-Condon factors. Spontaneous emission of the upper state is not explicitly included in the model, but will deserve special attention in the further analysis.

The dynamics of an *arbitrary* (degenerate as well as nondegenerate) three-level system arranged in the Λ configuration is best understood in the so-called dressed basis, where two lower states characterized by probability amplitudes g_0 and g'_0 are rotated as

$$\begin{pmatrix} B \\ D \end{pmatrix} = \begin{pmatrix} \sin(\theta/2) & \cos(\theta/2) \\ -\cos(\theta/2) & \sin(\theta/2) \end{pmatrix} \begin{pmatrix} g_0 \\ g'_i \end{pmatrix} \quad (43)$$

yielding amplitudes B and D of a bright and dark state, correspondingly, while the upper state amplitude a_0 remains unaffected. Here g'_i is amplitude of a given state from G' manifold (we shall use $i=0,2$). The dressing angle θ , sometimes called mixing angle [20] or dark area [21], is related to the original Rabi frequencies as $\sin(\theta/2)=\Omega_p/\Omega_B$ and $\cos(\theta/2)=\Omega_s/\Omega_B$, with bright field $\Omega_B=(\Omega_p^2+\Omega_s^2)^{1/2}$.

In the case of a degenerate system $\Omega_p=\Omega_s$, and the dressing angle θ in the transformation described by Eq. (43) becomes independent of the fields and equal to $\pi/2$. Also, $g'_i=g'_0$ in Eq. (43) since carrier frequencies of the fields are equal. The equations of motion in the dressed basis read

$$i \frac{d}{dt} \begin{pmatrix} B \\ a_0 \\ D \end{pmatrix} = \frac{1}{\sqrt{2}} \begin{pmatrix} 0 & \Omega & 0 \\ \Omega & 0 & 0 \\ 0 & 0 & 0 \end{pmatrix} \begin{pmatrix} B \\ a_0 \\ D \end{pmatrix}. \quad (44)$$

Clearly, the dynamics of the system is reduced to two-level physics where the population transfer is controlled by the integral of Rabi frequency over time, $\int dt \Omega(t)$, a quantity called pulse area. The dark state appears to be completely decoupled from the field, as indicated in Fig. 2(a). Recall that our goal is the complete transfer of population from state $|G, \bar{m}\rangle$ to state $|G', \bar{m}\rangle$, so that the probabilities evolve from $|g_0|^2=1$ to $|g'_0|^2=1$. The transfer dynamics in bare states corresponds to the excursion from $B=1$ to a_0 and back to $B=-1$ in the dressed state basis. In order to realize this transfer cycle the pulse area should take discrete values determined from equation

$$\int d\tau \Omega(\tau) = (2M+1)\sqrt{2}\pi, \quad (45)$$

where M is an integer. Evolution of populations in the degenerate three-level lambda system under the action of $\sqrt{2}\pi$ pulse is shown in Fig. 2(c). The only characteristic of the field which matters is its area. In accordance with the condition expressed by Eq. (45) and in line with the numerical simulation, such a pulse produces complete transfer. Note here that the transfer is critical to the value of the pulse area and thus requires a precise preparation scheme.

It is instructive for the moment to leave aside the three-level approximation and include surrounding states in the consideration, shown by thin lines in Fig. 2(a). Formally, we now allow all terms in sums of Eqs. (29) and (30) to participate in the dynamics. Practically, this is achieved by setting the nonmonochromaticity parameter R to a nonzero value. For sufficiently small values of the R parameter, increasing Rabi frequency while keeping the pulse-width constant results in well-pronounced quasiperiodic oscillations, depicted by the dashed curve in Fig. 2(d). Such periodicity is expected from the three-level considerations based on equations of motion, Eq. (42). For a larger value of the nonmonochromaticity parameter the increase in Rabi frequency eventually brings more and more vibrational states into play. As a consequence of this additional coupling, the transfer is no longer a periodic function of the Rabi frequency, as demonstrated

by the solid curve in Fig. 2(d). For even larger values of the Rabi frequency the transfer is no longer controllable. Note that plots in Fig. 2(d) are generated with accounting for the actual vibrational structure of the potential wells. Both solid and dashed curves indicate that the three-level approximation fails to correctly describe the dynamics when the field becomes strong.

B. Effects of dissipation

So far, dissipation effects have not been explicitly included in the model. A more rigorous approach would require to account for the effect of spontaneous emission from the upper state by including proper dissipation terms in equations of motion, Eq. (29)–(31). In general, such modification would require the formulation of a master equation for the density matrix instead of the Schrödinger equation for probability amplitudes. However, qualitative and even some quantitative estimates are already available without these complications, from the results reported above.

Clearly, the larger the population in the upper state the stronger the effect of dissipation. This guideline allows us to bypass the rigorous formalism and present a simple estimate. Transient population of the excited state exposes the atom to spontaneous decay for the time interval approximately equal to the pulse duration which is in our case approximately equal to the inverse pulse bandwidth $\Delta\omega^{-1}$. The probability of spontaneous emission $(\gamma/\Delta\omega)\max|a_0|^2$ is then estimated as the maximum population of the upper state weighted with the ratio of emission rate γ and $\Delta\omega$. Note that the atom after spontaneously emitting a photon has equal probability to move to the left as well as to the right. However, a 50% probability of success is too small to be called transfer. Moreover, the atom has comparable probabilities to appear in many different final vibrational states. This stochasticity destroys the deterministic character of the transfer which is our main goal.

There are two ways to diminish the effect of unwanted stochasticity associated with spontaneous emission. The first consists in using shorter pulses. The pulse shortening automatically yields an increase of the nonmonochromaticity parameter R . But then, many vibrational states are excited simultaneously. The drawback of having a distribution of excited states is that there is no known method for deterministic transfer of atomic wave packets.

The other way is to suppress the population transit through the upper state. It is important to notice that one-photon transitions play a significant role in the transfer, allowing for substantial transient population of the upper state; see Fig. 2(c). This indicates that spontaneous emission from the upper state can essentially affect the coherent dynamics and thus deteriorate the transfer of population. An effective way to suppress the one-photon processes is to give up the degenerate scheme and apply the pump and Stokes pulses in counterintuitive order [22], the method known as STIRAP (stimulated Raman adiabatic passage) [23].

C. STIRAP in the nondegenerate Λ scheme

In order to demonstrate STIRAP we turn to the nondegenerate three-level Λ system shown in Fig. 3(a), by allowing

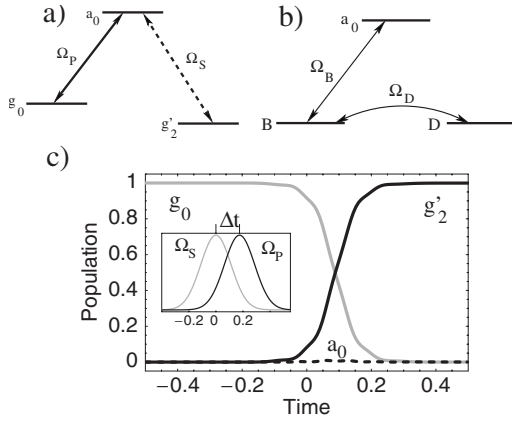


FIG. 3. STIRAP in a nondegenerate Λ system. (a) Bare states are coupled by the resonant pump and Stokes pulses of different carrier frequencies. (b) Dressed state picture of the Λ system. (c) Example of the STIRAP—the population transfer by the pump and Stokes pulses arranged in the counterintuitive order (Stokes precedes pump) as shown in the inset. Note the greatly suppressed population transit through the upper state as compared to the degenerate case in Fig. 2(c).

the two lower states $|G, \bar{m}\rangle$ and $|G', \bar{l}\rangle$ indicated by their probability amplitudes g_0 and g'_2 to have different quantum numbers: $\bar{m} \neq \bar{l}$. For that the pump and Stokes field should have different frequencies tuned in one- and two-photon resonance with the corresponding transitions. The equations of motion for the probability amplitudes of the vibrational states

$$i \frac{d}{dt} \begin{pmatrix} g_0 \\ a_0 \\ g'_2 \end{pmatrix} = \frac{1}{2} \begin{pmatrix} 0 & \Omega_P & 0 \\ \Omega_P & 0 & \Omega_S \\ 0 & \Omega_S & 0 \end{pmatrix} \begin{pmatrix} g_0 \\ a_0 \\ g'_2 \end{pmatrix} \quad (46)$$

are the obvious generalization of Eq. (42) to the case where the degeneracy of the fields is lifted.

The STIRAP technique is best understood in the dressed basis. We apply the dressing transformation to the two lower states as suggested in Eq. (43) and reformulate equations of motion (46) in terms of bright field Ω_B and dark field $\Omega_D = 2i(\Omega_S \dot{\Omega}_P - \Omega_P \dot{\Omega}_S) / \Omega_B^2$, where dot over a variable denotes the derivative with respect to time.

Finally, the equations of motion become

$$i \frac{d}{dt} \begin{pmatrix} B \\ a_0 \\ D \end{pmatrix} = \frac{1}{2} \begin{pmatrix} 0 & \Omega_B & -\Omega_D \\ \Omega_B & 0 & 0 \\ \Omega_D & 0 & 0 \end{pmatrix} \begin{pmatrix} B \\ a_0 \\ D \end{pmatrix}. \quad (47)$$

The dressed-state picture of states is shown in Fig. 3(b).

The idea of STIRAP is to arrange the atom-field interaction in such a manner that the system stays in the dark state during the population transfer from state g_0 to g'_2 that is formally equivalent to the requirement that the mixing angle θ in the rotation matrix of Eq. (43) evolves adiabatically from 0 to π . The transfer is accomplished by two pulses coming in the counterintuitive sequence—Stokes before

pump. As shown in Fig. 3(c), the complete population transfer takes place on the background of negligible transient population of the upper state.

STIRAP in Λ systems is well understood and offers full population transfer combined with the robustness to the pulse parameters, pulse shapes and overlap area of the pump and Stokes pulses. The problem is that this technique cannot be directly applied to the transfer of atoms in optical lattices even for vanishingly small R parameter. Formally, the structure of Franck-Condon factors does not allow us to single out only one state per manifold. On the contrary, the picture of interaction involves many states cross-coupled by both the pump and Stokes pulses, mainly because neighboring levels of deep wells are nearly equidistant. Strong fields that are necessary for the efficient transfer mix all the states in a complicated and not easily tractable manner. Probably, development of a learning type of algorithm for searching for optimal pulse shapes may be of some help for this sort of task [24]. However, even with such optimization schemes it is still a challenge to direct all, or almost all, population to a single eigenstate of the right well and accomplish this task bypassing the upper state. We choose a different strategy. In the next section we shall show how the problem can be reduced to a tractable number of states and analyzed analytically.

V. MODIFIED STIRAP IN OPTICAL LATTICES

The idea is to start with the conventional STIRAP technique, show its inapplicability, and propose a proper generalization to perform efficient atom transport. We first identify nine levels of interest, three per manifold, and then argue why the ladder allows such truncation.

A. Reduction to the nine-state system

Initially the atom is localized in the vibrational eigenstate $|G, \bar{m}\rangle$ characterized by the probability amplitude g_0 , as illustrated in Fig. 4(a). This state is coupled by the pump pulse to the upper state $|A, \bar{m}\rangle$ with associated probability amplitude a_0 . In its turn, the Stokes pulse couples the upper state to the lower state $|G', \bar{m} - \Delta n\rangle$ in the right well denoted by probability amplitude g'_2 . Here $\bar{m} - \Delta n$ is the quantum number of the eigenstate, with offset Δn to be chosen later on basing on the structure of Franck-Condon factors. The three states do not form a closed system. This conclusion immediately follows from parity considerations of the Franck-Condon factors. Thus we get the following equalities for dipole moments of (indicated in parenthesis) transitions:

$$d(g_1 \leftrightarrow a_1) = d(g'_1 \leftrightarrow a_1),$$

$$d(g_0 \leftrightarrow a_0) = d(g'_0 \leftrightarrow a_0),$$

$$d(g_2 \leftrightarrow a_2) = d(g'_2 \leftrightarrow a_2),$$

$$d(g_0 \leftrightarrow a_1) = -d(g'_0 \leftrightarrow a_1),$$

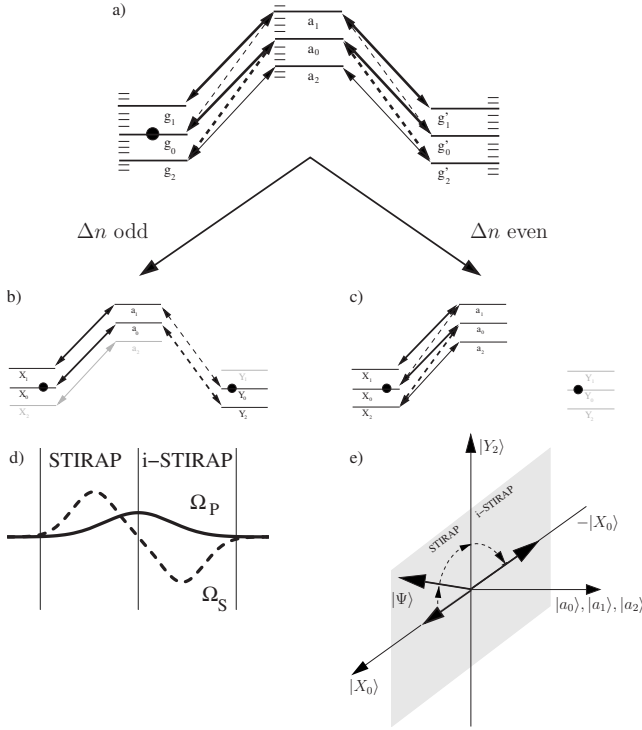


FIG. 4. The nine-level system for the population transfer between the three manifolds. (a) Bare state picture of the nine-level system with couplings produced by the pump (solid line) and Stokes (dashed line) pulse. Thick (thin) lines indicate strong (weak) transitions. Also shown are surrounding vibrational levels which ideally (for $R \rightarrow 0$) do not participate in the dynamics. The black circle represents the population initially concentrated in the g_0 state. (b) The nine-level system in the rotated basis, see Eq. (55), for odd offset Δn . The initial condition of $|g_0|^2 = 1$ corresponds to the population equally distributed between states X_0 and Y_0 . (c) Same as in (b) for even Δn . (d) The pulse sequence for the two-stage STIRAP: The conventional STIRAP sequence (Stokes precedes pump) is followed by the inverted STIRAP (pump precedes Stokes while the Stokes features an inverted sign). (e) Evolution of the state vector $|\Psi\rangle$ in the Hilbert space spanned by basis vectors $|X_0\rangle$, $|a_1\rangle$, $|a_0\rangle$, $|a_2\rangle$, and $|Y_2\rangle$. Under ideal STIRAP conditions the evolution of $|\Psi\rangle$ takes place mainly in the plane spanned by vectors $|X_0\rangle$ and $|Y_2\rangle$ with vanishing admixture of excited states. Note that the Hilbert space spanned by the five vectors is only a subspace of the original nine-dimensional Hilbert space. Since the projection on $|Y_0\rangle$ state (not shown) is constant in time and equal to $1/\sqrt{2}$, the length of the evolving reduced state vector in the five-dimensional space is $1/\sqrt{2}$. In the first stage the state vector is rotated from $X_0(-\infty) = 1/\sqrt{2}$ toward $|Y_2\rangle$. In the second stage the rotation proceeds farther toward $X_0(+\infty) = -1/\sqrt{2}$.

$$d(g_2 \leftrightarrow a_0) = -d(g'_2 \leftrightarrow a_0), \quad (48)$$

where probability amplitudes g_1 , g_2 , a_1 , a_2 , g'_1 , and g'_0 characterize states $|G, \bar{m} + \Delta n\rangle$, $|G, \bar{m} - \Delta n\rangle$, $|A, \bar{n} + \Delta n\rangle$, $|A, \bar{n} - \Delta n\rangle$, $|G', \bar{m} + \Delta n\rangle$, and $|G', \bar{m}\rangle$, respectively. We choose $\bar{n} \neq \bar{m}$. As follows from equalities Eqs. (48), the coupling strength of the upper state a_0 to lower states g_2 and g'_0 is the same as to g'_2 and g_0 in the ideal STIRAP three-level configuration. Therefore, taking only three states into account is

not sufficient and the evolution of at least five states must be considered simultaneously.

In its turn, this five-level configuration is coupled to the other four levels by the same pump and Stokes fields along transitions indicated by thin lines in Fig. 4(a). These transitions are resonant with corresponding fields and the magnitude of the couplings depends on frequencies of applied fields. The frequency difference of the pump and Stokes field controls the offset Δn which defines frequency separation $\Delta n\nu$ of the two closest resonant levels within each manifold.

It is in our interest to restrict the analysis to a minimal number of participating levels, that is, to keep the outgoing transitions as weak as possible. From the Franck-Condon pattern in Fig. 1(c) plotted for transitions between the eigenstate $|G, \bar{m} = 43\rangle$ in the lower left manifold and states $|A, n\rangle$ in the upper manifold, we choose the central state a_0 with $\bar{n} = 48$ which is most strongly coupled. The closest eigenstate which appears least coupled to $|G, \bar{m}\rangle$ is given by $|A, \bar{n} = 55\rangle$. This coupling is approximately 10 times weaker. Thus states of maximal and minimal coupling in the excited manifold are separated by the offset $\Delta n = 7$. Symmetry arguments, Eqs. (48), predict an equally weak coupling for the transition $g'_0 \leftrightarrow a_1$. Later we will see that an order of magnitude difference in coupling strength causes about 10% transient population of the state a_1 . This value is of the same order as the transfer via a_0 . As a consequence we include the transition $g_0 \leftrightarrow a_1$ in the minimal model even though it is 10 times weaker than the dominant transition $g_0 \leftrightarrow a_0$.

Unlike the one-photon coupling of states a_0 and a_1 to the initially populated state g_0 , the state a_2 is coupled to g_0 via a three-photon transition. Moreover, an analysis of the Franck-Condon factors (not shown) which describe the coupling of the eigenstate g_2 to eigenstates in the upper manifold show that the state a_2 is only weakly coupled, more precisely, 22 times weaker than the dominant transition $g_0 \leftrightarrow a_0$. So, we can safely ignore the passage of population through the upper state a_2 .

B. Reduced equations of motion

Thus, by the judicious choice of the frequencies of applied fields the complicated ladder of couplings is reduced to a six-level system with two states per manifold:

$$g_0, g_2 \leftrightarrow a_1, a_0 \leftrightarrow g'_0, g'_2.$$

Nevertheless we keep all nine states in the consideration to further demonstrate the insignificance of couplings to the other levels. The state vector is defined by nine probability amplitudes

$$\Phi = (g_1, g_0, g_2, a_1, a_0, a_2, g'_1, g'_0, g'_2)^T. \quad (49)$$

The equation of motion in matrix form

$$i \frac{d}{dt} \Phi = \mathbf{M}_\Phi \Phi \quad (50)$$

is the truncated version of the system of equations (29)–(31). Here, the coupling matrix reads

$$\mathbf{M}_\Phi = \begin{pmatrix} \mathbf{0} & \Omega_+^T & \mathbf{0} \\ \Omega_+ & \mathbf{0} & \Omega_- \\ \mathbf{0} & \Omega_-^T & \mathbf{0} \end{pmatrix} \quad (51)$$

with $\mathbf{0}$ representing a zero matrix of the dimension 3×3 and with the field block matrices

$$\Omega_\pm = \Omega_P \pm \Omega_S, \quad (52)$$

where

$$\Omega_P = \frac{1}{\hbar} \begin{pmatrix} \tilde{d}_{11}E_P & 0 & 0 \\ 0 & \tilde{d}_{00}E_P & 0 \\ 0 & 0 & \tilde{d}_{22}E_P \end{pmatrix} \quad (53)$$

and

$$\Omega_S = \frac{1}{\hbar} \begin{pmatrix} 0 & \tilde{d}_{01}E_S & 0 \\ 0 & 0 & \tilde{d}_{20}E_S \\ 0 & 0 & 0 \end{pmatrix}. \quad (54)$$

The upper index T denotes the matrix transposition. Dipole moments $\tilde{d}_{ij} = d(g_i \leftrightarrow a_j)$ are introduced to simplify notations. Symmetry properties expressed by Eqs. (48) are taken into account by writing the block matrices in Eqs. (53) and (54).

The coupling matrix \mathbf{M}_Φ is highly symmetric and allows for further simplification. It turns out that a linear transformation of two vibrational eigenstates belonging to the two lower manifolds and having equal quantum numbers reduces the problem even further. This transformation (rotation) is given by

$$X_i = \frac{1}{\sqrt{2}}(g_i + g'_i) \quad (55)$$

and

$$Y_i = \frac{1}{\sqrt{2}}(g_i - g'_i), \quad (56)$$

with $i=0,1,2$. The state vector in the rotated basis is described by nine probability amplitudes arranged in vector form

$$\Psi = (X_1, X_0, X_2, a_1, a_0, a_2, Y_1, Y_0, Y_2)^T. \quad (57)$$

The equation of motion in matrix form reads

$$i \frac{d}{dt} \Psi = \mathbf{M}_\Psi \Psi \quad (58)$$

with the field matrix

$$\mathbf{M}_\Psi = \begin{pmatrix} \mathbf{0} & \Omega_P & \mathbf{0} \\ \Omega_P & \mathbf{0} & \Omega_S \\ \mathbf{0} & \Omega_S^T & \mathbf{0} \end{pmatrix}. \quad (59)$$

Figure 4(b) demonstrates the resulting scheme of levels. Three states appear to be decoupled from the rest system while the other six form two separate lambda schemes. It is remarkable how simple the picture becomes in the rotated

basis. The simplified coupling pattern allows us to draw conclusions that were not obvious in the bare basis. Thus the interference of different paths in the nine-level system results in a fully decoupled upper state a_2 . Even if the dipole moments $g_2 \leftrightarrow a_2$ and $g'_2 \leftrightarrow a_2$ had appreciable values we would not get a population transfer via a_2 state anyway. The only important step was the choice of transitions $g_0 \leftrightarrow a_1$ and $g'_0 \leftrightarrow a_1$ to be weak that allowed us to truncate the ladder from above.

C. Inverted STIRAP

Let us recall that our goal is to fully transfer the population from the g_0 state to one of the eigenstates in the adjacent well. In the nine-level configuration the choice is between g'_2 , g'_0 , or g'_1 . The latter can be populated only via the weakly coupled state a_1 and is therefore excluded from the consideration. The state g'_2 cannot be fully populated since $X_2=0$ holds at all times, for the reason that X_2 is decoupled from the evolution. So, the final state can only be the state g'_0 .

Initial conditions in the rotated basis are illustrated in Fig. 4(b) by two black circles of equal size, that is

$$X_0(-\infty) = Y_0(-\infty) = \frac{1}{\sqrt{2}}. \quad (60)$$

The state Y_0 is weakly coupled to the upper state a_1 . Therefore during the evolution a loss of population from this state is negligible, and the upper lambda configuration can be excluded from the analysis. In the lower Λ scheme a full population transfer from g_0 to g'_0 is compatible with the condition $Y_0(t) = \text{const} = 1/\sqrt{2}$ only when $X_0(-\infty) = 1/\sqrt{2}$ evolves under the action of the pump and Stokes fields into $X_0(+\infty) = -1/\sqrt{2}$.

Note that the above analysis refers to cases where the offset Δn covers an odd number of vibrational states. When Δn is even the interaction pattern changes, compare schemes in Fig. 4(b) and Fig. 4(c). This difference originates from the alternation of signs of Franck-Condon factors for transitions with unity change in the sum of quantum numbers, see Eq. (40), for instance if the dipole moment for transition $|G, \bar{m}\rangle \leftrightarrow |A, \bar{n}\rangle$ is positive then for transition $|G, \bar{m}\rangle \leftrightarrow |A, \bar{n} \pm 1\rangle$ it is negative. For even Δn the scheme again consists of two lambda systems one of which, $X_0 \leftrightarrow a_1 \leftrightarrow X_1$, is excluded from the analysis on the basis of weak $X_0 \leftrightarrow a_1$ coupling. For the residual lambda system, $X_0 \leftrightarrow a_0 \leftrightarrow X_2$, the analysis will follow the same lines as presented below.

We see that the five-level system in the bare basis is reduced in the rotated basis to a three-level Λ configuration $X_0 \leftrightarrow a_0 \leftrightarrow Y_2$ in Fig. 4(b). The application of the standard STIRAP method allows us to transfer the population from X_0 to Y_2 . However, this step alone is not sufficient. Our goal is to return to the state $X_0 e^{i\phi}$ with phase flip $\phi = \pi$. For that we need a second stage where two pulses are arranged in the sequence which we call inverted STIRAP (i-STIRAP). In this sequence the order is intuitive—the pump pulse is followed by the Stokes pulse. Furthermore, the Stokes pulse features an inverted sign. The complete pulse sequence is shaped as illustrated in Fig. 4(d). The two-stage evolution of

states in the rotated basis follows the scheme

$$\begin{cases} X_0 = \frac{1}{\sqrt{2}} \\ Y_0 = \frac{1}{\sqrt{2}} \\ Y_2 = 0 \end{cases} \xrightarrow{\text{STIRAP}} \begin{cases} X_0 = 0 \\ Y_0 = \frac{1}{\sqrt{2}} \\ Y_2 = -\frac{1}{\sqrt{2}} \end{cases} \xrightarrow{\text{i-STIRAP}} \begin{cases} X_0 = -\frac{1}{\sqrt{2}} \\ Y_0 = \frac{1}{\sqrt{2}} \\ Y_2 = 0 \end{cases}. \quad (61)$$

The same scheme in the bare basis reads

$$\begin{cases} g_0 = 1 \\ g'_0 = 0 \\ g_2 = 0 \\ g'_2 = 0 \end{cases} \xrightarrow{\text{STIRAP}} \begin{cases} g_0 = 1/2 \\ g'_0 = -1/2 \\ g_2 = -1/2 \\ g'_2 = 1/2 \end{cases} \xrightarrow{\text{i-STIRAP}} \begin{cases} g_0 = 0 \\ g'_0 = -1 \\ g_2 = 0 \\ g'_2 = 0 \end{cases}. \quad (62)$$

This idealized transfer scheme implies that the dynamics occurs adiabatically and the population stays in the dark state (composed of X_0 and Y_2) at all times. Then, the state vector evolves as shown in Fig. 4(e). The dressing angle θ spans an entire circle from 0 to 2π , while in standard STIRAP arrangement θ covers only a semicircle.

The adiabaticity requires strong fields. At the same time they should not initiate substantial population transfer via neighboring vibrational states. As noted earlier, the necessary condition for that is the relative monochromaticity of the applied fields, expressed by the R parameter. We choose a small value of R and perform two sets of numerical runs with pump and Stokes pulses of Gaussian shapes

$$\Omega_P = \Omega_{P0} \exp\left[-\frac{1}{2}\left(\frac{t}{T_P}\right)^2\right], \quad (63)$$

and

$$\Omega_S = \Omega_{S0} \exp\left[-\frac{1}{2}\left(\frac{t+\Delta t}{T_S}\right)^2\right] - \Omega_{S0} \exp\left[-\frac{1}{2}\left(\frac{t-\Delta t}{T_S}\right)^2\right]. \quad (64)$$

The peak amplitudes Ω_{P0} and Ω_{S0} as well as the separation Δt are optimized to reach the best performance. Figure 5 shows results with and without accounting for surrounding vibrational states. The goal is reached—the atom is transferred to the adjacent well with high probability. The atom appears in the vibrational eigenstate with the same quantum number as the initial state. The transfer to large extent bypasses states in the upper manifold so that spontaneous emission has less chance to influence the deterministic evolution when compared to the case of degenerate fields. The results of the full scale numerical analysis with 30 surrounding vibrational states indicate that Raman-induced heating processes are not present in our transfer scheme at all stages of the evolution.

Calculations with deeper optical potentials (not shown) suggest even better suppression of population transit through the upper states. The present calculations are based on the characteristic parameters of the optical lattice taken from the

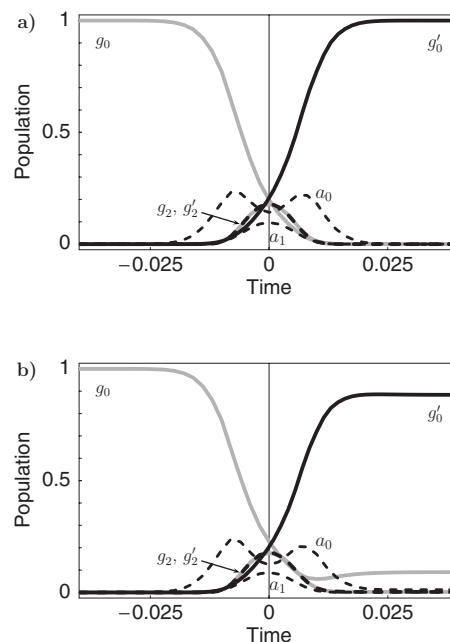


FIG. 5. Dynamics of populations of relevant vibrational states in the optical lattice. Parameters are $\Omega_{P0} = \Omega_{S0} = 0.07$, $T_P = 16$, $T_S = 6.4$, and $\Delta t = 11$. Franck-Condon factors are chosen as explained in the text. (a) Nine-level system of Fig. 4(a), $R \rightarrow 0$. (b) Same as (a) taking into account 30 surrounding vibrational states in each well of the optical lattice, $R = 0.01$. Amplitude a_2 is not shown; no population is transiting via a_2 due to absence of coupling; see Fig. 4(b).

experiment [26] on cold atoms in a high- Q ring cavity. On the other hand, shallow potentials are not favorable for the efficient transfer.

VI. DISCUSSION

The technique proposed here provides a prescription of deterministic transfer of single atoms through an optical lattice. Given an atom that is initially prepared in a vibrational eigenstate in one well of the periodic potential, the goal is to move it to the adjacent well with probability close to one. The process is controlled by two strong optical fields tuned in resonance with an internal atomic transition. Though the fields are resonant and strong we nevertheless pose the additional condition that the excursion of the atom through the upper electronic state is suppressed so that the atom is not exposed to the undesirable effect of spontaneous emission. In this requirement we are inspired by the STIRAP method of transferring population between two lower states in a three-level system of Λ configuration while bypassing the upper state.

Instead of three internal atomic states our model deals with three manifolds in each of which the ladder of vibrational states is characterized by approximately equal frequency steps. In such system it is not possible to separate three states coupled by two nondegenerate optical fields. As shown, at least five states participate in the dynamics. However, due to symmetry relations imposed on Franck-Condon factors, the three-level Λ configuration is recovered in the

rotated basis. In this Λ scheme the transfer of the atom to the adjacent well corresponds to a full cycle of population transfer between the two lower states and returning to the initial state with the opposite sign of the probability amplitude. As the standard STIRAP realizes only half of the cycle, for the second semicycle we propose a modification of the STIRAP technique called here inverted STIRAP. The essence of the method is in application of the pump and Stokes fields in the intuitive order (pump precedes Stokes) with the inverted sign of the Stokes pulse. Numerical results demonstrate that the combination of the STIRAP and the inverted STIRAP fulfills the task of atom transfer to the adjacent well with high fidelity while suppressing transient population of the atomic excited state.

The term STIRAP used here should be interpreted in a broader sense than simply the population transfer between internal atomic states. Optical fields simultaneously influence the external degrees of freedom, thus affecting the position of the atom. The generalization of STIRAP to the control of molecular motion was discussed in some detail by Garraway and Suominen in Ref. [25]. In the spirit of their argumentation, the action of the Raman pulse can be viewed as a transient light-induced potential imposed on the steady-state potential of the optical lattice. This time-dependent potential forces the atom to move along a designed trajectory and makes it finally arrive at the adjacent well. Relatively long pulses (corresponding to small value of R parameter) assure that the motion is slow. The characteristic “slow” is to emphasize the fact that the transfer time is large compared to the vibrational period.

The combination of STIRAP and inverted STIRAP serves as the most effective transfer mechanism as long as the evolution can be restricted in the rotated basis to the ideal three-level configuration. Involving neighboring vibrational states in the dynamics destroys the population transfer. The efficiency is therefore a sensitive function of the pulse bandwidth which should be as small as possible to approach the idealized scenario. For wider bandwidths, the existence of a dark state and more general, conditions for the optimal transfer, remain open questions (note relevant studies [27–30]).

Another interesting issue is the population transfer via a continuum of states. This situation is realized for the practically interesting example when the atom is initially localized in the lowest vibrational state, i.e., in the bottom of the left potential well. Here the scenario is expected to be the same as discussed in the paper: The atom gets a momentum kick from a Raman pulse, moves toward the right well, then gets decelerated by another Raman pulse, and finally (ideally) appears in the lowest eigenstate of the right well.

A more complicated situation arises with the transfer of broad atomic wave packets, i.e., when initially many vibrational states are simultaneously excited in the left potential well. A possible problem here is caused by the inhomogeneous structure of the Franck-Condon pattern. The coupling strength differs from state to state and those states that are too weakly coupled by the Raman pulse do not participate in the transfer. So, most likely the transferred wave packet deteriorates during the transportation.

As a concluding remark, we note that some aspects of our analysis of the population transfer in the multilevel environment and the generalization of the STIRAP technique can be useful in the context of coherent control of molecular motion and distillation of enantiomers [31,32]. It is also interesting to draw a parallel with the method of transfer of neutral atoms among dipole traps via tunneling based on three-level optics analogy [33]. Finally, extensions of the STIRAP technique [34–36] to create a superposition of multilevel states naturally leads to the notion of coherent superposition of vibrational states belonging to two spatially separated wells (Schrödinger cat states).

ACKNOWLEDGMENTS

V.V.K. wishes to thank the Alexander von Humboldt Stiftung for financial support and the opportunity to work at the University of Ulm. W.M. and W.P.S. acknowledge financial support by the Landesstiftung Baden-Württemberg. Moreover, W.P.S. also would like to thank the Alexander von Humboldt Stiftung and the Max-Planck-Gesellschaft for financial support.

-
- [1] S. Rolston, *Phys. World* **11**(10), 27 (1998), for example.
 - [2] P. S. Jessen and I. H. Deutsch, *Adv. Mol. Opt. Phys.* **37**, 95 (1996), and references therein.
 - [3] I. H. Deutsch and P. S. Jessen, *Phys. Rev. A* **57**, 1972 (1998).
 - [4] L. Guidoni and P. Verkerk, *J. Opt. B: Quantum Semiclassical Opt.* **1**, R23 (1999).
 - [5] I. Bouchoule, H. Perrin, A. Kuhn, M. Morinaga, and C. Salomon, *Phys. Rev. A* **59**, R8 (1999).
 - [6] R. Eijnisman, P. Rudy, H. Pu, and N. P. Bigelow, *Phys. Rev. A* **56**, 4331 (1997).
 - [7] M. BenDahan, E. Peik, J. Reichel, Y. Castin, and C. Salomon, *Phys. Rev. Lett.* **76**, 4508 (1996).
 - [8] M. Raizen, C. Salomon, and Q. Niu, *Phys. Today* **50**(7), 30 (1997).
 - [9] R. Abfalterer, C. Keller, S. Bernet, M. K. Oberthaler, J. Schmiedmayer, and A. Zeilinger, *Phys. Rev. A* **56**, R4365 (1997).
 - [10] D. Jaksch, H.-J. Briegel, J. I. Cirac, C. W. Gardiner, and P. Zoller, *Phys. Rev. Lett.* **82**, 1975 (1999).
 - [11] G. K. Brennen, C. M. Caves, P. S. Jessen, and I. H. Deutsch, *Phys. Rev. Lett.* **82**, 1060 (1999).
 - [12] S. Marksteiner, K. Ellinger, and P. Zoller, *Phys. Rev. A* **53**, 3409 (1996).
 - [13] H. Katori, S. Schlipf, and H. Walther, *Phys. Rev. Lett.* **79**, 2221 (1997).
 - [14] P. M. Visser and G. Nienhuis, *Phys. Rev. A* **56**, 3950 (1997).
 - [15] C. Mennerat-Robilliard, D. Lucas, S. Guibal, J. Tabosa, C. Jurczak, J. Y. Courtois, and G. Grynberg, *Phys. Rev. Lett.* **82**, 851 (1999).
 - [16] M. Schiavoni, L. Sanchez-Palencia, F. Renzoni, and G. Gryn-

- berg, Phys. Rev. Lett. **90**, 094101 (2003).
- [17] O. Mandel, M. Greiner, A. Widera, T. Rom, T. W. Hänsch, and I. Bloch, Phys. Rev. Lett. **91**, 010407 (2003).
- [18] S. Kuhr, W. Alt, D. Schrader, I. Dotsenko, Y. Miroshnychenko, W. Rosenfeld, M. Khudaverdyan, V. Gomer, A. Rauschenbeutel, and D. Meschede, Phys. Rev. Lett. **91**, 213002 (2003).
- [19] The nonvanishing electric field in the tails results in little probability for the atom to penetrate into wells other than the desired one. Such transitions deteriorate the transfer efficiency. One method to suppress them is to use transfer pulses of super-Gaussian transverse shape. A more detailed discussion would require position-dependent fields and is beyond the present study.
- [20] M. Fleischhauer and A. S. Manka, Phys. Rev. A **54**, 794 (1996).
- [21] J. H. Eberly and V. V. Kozlov, Phys. Rev. Lett. **88**, 243604 (2002).
- [22] J. Oreg, F. T. Hioe, and J. H. Eberly, Phys. Rev. A **29**, 690 (1984).
- [23] K. Bergmann, H. Theuer, and B. Shore, Rev. Mod. Phys. **70**, 1003 (1998).
- [24] H. Rabitz, R. de Vivie-Riedle, M. Motzkus, and K. Kompa, Science **288**, 824 (2000).
- [25] B. M. Garraway and K.-A. Suominen, Phys. Rev. Lett. **80**, 932 (1998).
- [26] D. Kruse, M. Ruder, J. Benhelm, C. von Cube, C. Zimmermann, P. W. Courteille, Th. Elsässer, B. Nagorny, and A. Hemmerich, Phys. Rev. A **67**, 051802(R) (2003).
- [27] N. Vitanov, B. W. Shore, and K. Bergmann, Eur. Phys. J. D **4**, 15 (1998).
- [28] N. V. Vitanov and S. Stenholm, Phys. Rev. A **60**, 3820 (1999).
- [29] P. Pillet, C. Valentin, R.-L. Yuan, and J. Yu, Phys. Rev. A **48**, 845 (1993).
- [30] C. Valentin, J. Yu, and P. Pillet, J. Phys. II **4**, 1925 (1994).
- [31] M. Shapiro, E. Frishman, and P. Brumer, Phys. Rev. Lett. **84**, 1669 (2000).
- [32] M. Shapiro, E. Frishman, and P. Brumer, Phys. Rev. Lett. **91**, 129902(E) (2003).
- [33] K. Eckert, M. Lewenstein, R. Corbalán, G. Birkel, W. Ertmer, and J. Mompart, Phys. Rev. A **70**, 023606 (2004).
- [34] P. Marte, P. Zoller, and J. L. Hall, Phys. Rev. A **44**, R4118 (1991).
- [35] N. V. Vitanov, K.-A. Suominen, and B. W. Shore, J. Phys. B **32**, 4535 (1999).
- [36] Y. Niu, S. Gong, R. Li, and S. Jin, Phys. Rev. A **70**, 023805 (2004).